

A Highly Reactive P450 Model Compound I

Seth R. Bell and John T. Groves*

Department of Chemistry, Princeton University, Princeton, New Jersey 08544

Received April 27, 2009; E-mail: jtgroves@princeton.edu

The substrate oxygenation reactions mediated by cytochrome P450 proteins comprise many key transformations in steroid biosynthesis and drug metabolism. Significant advances in heme-protein enzymology,¹ the characterization of synthetic model compounds,² and computational approaches³ have pointed to a reactive oxoiron(IV)–porphyrin π -radical cation in the consensus mechanism. Compound I model compounds, such as the thoroughly characterized $[\text{OFe}^{\text{IV}}\text{-TMP}]^+$,^{4,5} have exhibited a full range of oxygen transfer reactions.⁶ However, the low kinetic reactivity of $[\text{OFe}^{\text{IV}}\text{-TMP}]^+$ has left unanswered just how the protein manages to generate a sufficiently reactive intermediate and what that reactive species is.^{7–10} We have shown that cationic oxomanganese(V)–porphyrin complexes such as $\text{OMn}^{\text{V}}\text{-4-TMPyP}$ display very high rates for oxygen transfer reactions in aqueous solution.^{11,12} Here we report the detection and kinetic characterization of $[\text{OFe}^{\text{IV}}\text{-4-TMPyP}]^+$, which shows extraordinary rates for C–H hydroxylations.

The reaction of $\text{Fe}^{\text{III}}\text{-4-TMPyP}$ with *m*CPBA was analyzed by stopped-flow spectrophotometry, as we have previously described.^{11,13} As can be seen in the UV–vis spectral time course (Figure 1), the starting iron(III)–porphyrin spectrum (λ_{max} 421 nm) was completely transformed within 20 ms into that of a new intermediate, **1**, displaying a weak, blue-shifted Soret band at 402 nm and an absorbance at 673 nm, typical of a porphyrin π -radical cation.^{4,14} Accordingly, we assigned the $[\text{OFe}^{\text{IV}}\text{-4-TMPyP}]^+$ formulation to **1**. Global analysis afforded a second-order rate constant $k_1 = (1.59 \pm 0.06) \times 10^7 \text{ M}^{-1} \text{ s}^{-1}$ for the appearance of **1**. In a slower, subsequent phase of the reaction (Scheme 1), **1** was transformed into the well-characterized $\text{OFe}^{\text{IV}}\text{-4-TMPyP}$ (λ_{max} 427 nm; $k_2 = 8.8 \pm 0.1 \text{ s}^{-1}$).^{15–17} Isosbestic points for the conversion of **1** to $\text{OFe}^{\text{IV}}\text{-4-TMPyP}$ were apparent at 413 and 570 nm. This transformation was more rapid at higher pH, in contrast to the behavior of the corresponding $\text{OMn}^{\text{V}}\text{-4-TMPyP}$ complex.^{11,18}

Intermediate **1** was found to be very highly reactive toward C–H bond hydroxylations. Slow addition of *m*CPBA to a solution of 5 mM xanthene and 50 μM $\text{Fe}^{\text{III}}\text{-4-TMPyP}$ was monitored by ¹H and ¹³C NMR spectroscopy. The major product, 9-xanthanol (H9, δ 5.75; C9, δ 62), was formed in 90% yield based on added oxidant (Figure S1 in the Supporting Information). A small amount of xanthone was also formed. The Fe^{III} catalyst was recovered with negligible decomposition. Significantly, when the oxidation was carried out in 47.5% ¹⁸O₂, electrospray ionization mass spectrometry of the 9-xanthanol product indicated 21% ¹⁸O incorporation (m/z 199/197 = 0.27). This partial exchange is consistent with an oxygen-rebound reaction scenario with \sim 50% dilution of the ¹⁶O-peroxyacid-derived oxygen with ¹⁸O water occupying the second axial ligation site.^{19,20} Xanthene/xanthene-*d*₂ (1:1) revealed a modest kinetic isotope effect, $k_{\text{H}}/k_{\text{D}} = 2.1$ (m/z 197/198).

Since the oxidation of $\text{Fe}^{\text{III}}\text{-4-TMPyP}$ by *m*CPBA was so fast, we could conveniently monitor the kinetics of the reaction of **1** with xanthene using a single-mixing stopped-flow experiment (Figure 2A). Global analysis of the spectral data produced a rate constant $k_3 = (3.6 \pm 0.3) \times 10^6 \text{ M}^{-1} \text{ s}^{-1}$. A similar value was

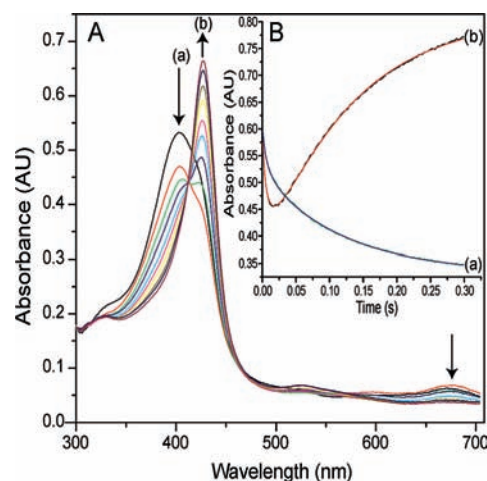
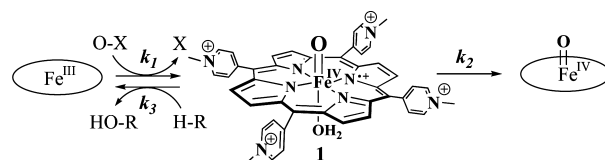


Figure 1. (A) UV–vis transients observed upon mixing of 10 μM $\text{Fe}^{\text{III}}\text{-4-TMPyP}$ with 3 equiv of *m*CPBA at pH 4.7, 10.0 °C. (B) Data obtained at (a) 402 and (b) 427 nm and the superimposed global fits.

Scheme 1. Kinetic Partitioning of $[\text{OFe}^{\text{IV}}\text{-4-TMPyP}]^+$ (**1**) between Spontaneous Decay to $\text{OFe}^{\text{IV}}\text{-4-TMPyP}$ (k_2) and Substrate Hydroxylation Resulting in the Formation of $\text{Fe}^{\text{III}}\text{-4-TMPyP}$ (k_3)



obtained by monitoring at 673 nm (Figure 2A). Control experiments showed that $\text{OFe}^{\text{IV}}\text{-4-TMPyP}$ had negligible reactivity toward xanthene over this time course.

Reactions of fluorene-4-carboxylic acid and 4-isopropyl- and 4-ethylbenzoic acid with **1** also gave very high rates for C–H hydroxylation, with second-order rate constants of $(1.80 \pm 0.06) \times 10^5$, $(9.0 \pm 0.2) \times 10^3$, and $(7.5 \pm 0.1) \times 10^3 \text{ M}^{-1} \text{ s}^{-1}$, respectively. The corresponding alcohol products were formed in each case. These reactions are remarkably fast, and as can be seen in Figure 2B, the rates correlated well with the scissile C–H bond dissociation energy (BDE), indicating a homolytic hydrogen abstraction transition state.²¹ Reaction of **1** with bromide ion afforded hypobromite with $k_3 = (3.14 \pm 0.04) \times 10^5 \text{ M}^{-1} \text{ s}^{-1}$.¹³

These results show that $[\text{OFe}^{\text{IV}}\text{-4-TMPyP}]^+$ (**1**), which is accessed chemically from a peroxide precursor, is orders of magnitude more reactive than the well-studied tetramesityl analogues.^{4,6,7,9} Mapping the rate constants observed here for C–H bond cleavage by **1** onto the Brønsted–Evans–Polanyi relationship^{21,22} for similar substrates (as shown in the Table of Contents graphic) yielded an estimate of \sim 100 kcal/mol for the BDE of H– $\text{OFe}^{\text{IV}}\text{-4-TMPyP}$; this is much larger than the values estimated for H– $\text{OFe}^{\text{IV}}\text{-TMP}$ (92 kcal/mol)⁷ and H– $\text{OFe}^{\text{III}}\text{-TPFP}$ (\sim 86

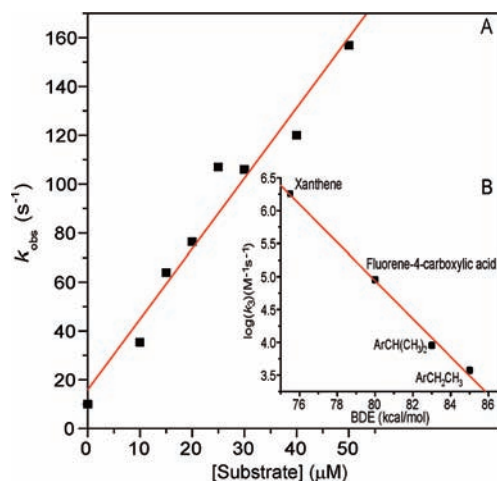


Figure 2. (A) Observed rate constant k_{obs} at 673 nm vs [xanthene] for the oxidation by **1** at pH 4.7, 14.5 °C, yielding $k_3 = (2.8 \pm 0.3) \times 10^6 \text{ M}^{-1} \text{ s}^{-1}$. (B) Correlation of k_3 with C–H bond dissociation energy.

kcal/mol).²³ Indeed, **1** showed a rate constant for ethylbenzoic acid hydroxylation similar to that reported recently by Newcomb and co-workers²⁴ for ethylbenzene with CYP119 and chloroperoxidase compound I.

The interesting question is *why* synthetic OFe^{IV}–porphyrin π -radical cations should have such a great variability in their intrinsic reactivities. We have shown that electron-withdrawing meso substituents dramatically *decrease* the reactivity of oxoMn^V–porphyrins.¹¹ The effects have been traced to stabilization of the singlet d^2 ground state with respect to the triplet and quintet manifolds, stabilization of the porphyrin HOMO, and the unique centrosymmetric *trans*-dioxo ligand arrangement.²⁵ Clearly, the situation for iron described here is markedly different. A relatively high redox potential for porphyrin ring oxidation is expected for Fe^{III}–4-TMPyP. Further, efficient transmission of the electron deficit to the metal core is assured by the large orbital coefficients on the meso carbon and the pyrrole nitrogens in the a_{2u} porphyrin HOMO. Indeed, the pK_a of the axial water in diaquaFe^{III}–4-TMPyP is only 5.5, while the corresponding acidity of diaquaFe^{III}–TMPS is 7.5.²⁶ Density functional theory calculations have shown that reaction barriers in oxo transfer reactions may be lowered by decreasing the energy gaps to higher-spin configurations for both manganese^{25,27} and iron.^{22,28} A decrease in the σ -donor properties of the coordinating pyrrole nitrogens due to the meso substituent would be expected to *decrease* the energy of the iron $d_{x^2-y^2}$ orbital. The high-spin state of an unsubstituted oxoFe^{IV}–porphyrin radical cation, with the iron $d_{x^2-y^2}$ orbital singly occupied, has been calculated to be only 14 kcal/mol above the nearly degenerate doublet and quartet ground-state structures.²⁹ We suggest that the high kinetic reactivity observed here experimentally for **1** may result from both a low-lying a_{2u} porphyrin HOMO and facilitated spin-state crossing phenomena in the course of the reaction. More generally, the results

suggest that even subtle charge modulation at the heme active site of P450 to accomplish a similar tuning of state-crossing energies or lower stability of the porphyrin π -radical cation could result in high reactivity of a cytochrome P450 compound I.

Acknowledgment. Support of this research by the National Institutes of Health (R37-GM36298) and the National Science Foundation (CHE 0316301) is gratefully acknowledged.

Supporting Information Available: Experimental details and NMR data (Figure S1). This material is available free of charge via the Internet at <http://pubs.acs.org>.

References

- (1) Ortiz de Montellano, P. R.; De Voss, J. J. In *Cytochrome P450 Structure, Mechanism and Biochemistry*, 3rd ed.; Ortiz de Montellano, P. R., Ed.; Kluwer Academic/Plenum: New York, 2005; pp 183–245.
- (2) Groves, J. T. In *Cytochrome P450: Structure, Mechanism, and Biochemistry*, 3rd ed.; Ortiz de Montellano, P. R., Ed.; Kluwer Academic/Plenum: New York, 2005; pp 1–44.
- (3) Shaik, S.; Hirao, H.; Kumar, D. *Acc. Chem. Res.* **2007**, *40*, 532–542.
- (4) Groves, J. T.; Haushalter, R. C.; Nakamura, M.; Nemo, T. E.; Evans, B. J. *J. Am. Chem. Soc.* **1981**, *103*, 2884–2886.
- (5) Abbreviations: TMP, 5,10,15,20-tetramesitylporphyrin; 4-TMPyP, 5,10,15,20-tetrakis(*N*-methyl-4-pyridinium)porphyrin; *m*CPBA, *m*-chloroperoxybenzoic acid; TMPS, 5,10,15,20-tetramesityloctasulfonate.
- (6) Groves, J. T.; Watanabe, Y. *J. Am. Chem. Soc.* **1988**, *110*, 8443–8452.
- (7) Pan, Z. Z.; Zhang, R.; Fung, L. W. M.; Newcomb, M. *Inorg. Chem.* **2007**, *46*, 1517–1519.
- (8) Pan, Z. Z.; Wang, Q.; Sheng, X.; Horner, J. H.; Newcomb, M. *J. Am. Chem. Soc.* **2009**, *131*, 2621–2628.
- (9) Franke, A.; Fertinger, C.; van Eldik, R. *Angew. Chem., Int. Ed.* **2008**, *47*, 5238–5242.
- (10) Takahashi, A.; Kurahashi, T.; Fujii, H. *Inorg. Chem.* **2009**, *48*, 2614–2625.
- (11) Jin, N.; Groves, J. T. *J. Am. Chem. Soc.* **1999**, *121*, 2923–2924.
- (12) Groves, J. T.; Lee, J. B.; Marla, S. S. *J. Am. Chem. Soc.* **1997**, *119*, 6269–6273.
- (13) Lahaye, D.; Groves, J. T. *J. Inorg. Biochem.* **2007**, *101*, 1786–1797.
- (14) Mandon, D.; Weiss, R.; Jayaraj, K.; Gold, A.; Ternier, J.; Bill, E.; Trautwein, A. X. *Inorg. Chem.* **1992**, *31*, 4404–4409.
- (15) Lee, J. B.; Hunt, J. A.; Groves, J. T. *J. Am. Chem. Soc.* **1998**, *120*, 7493–7501.
- (16) Bell, S. E. J.; Cooke, P. R.; Inchley, P.; Leanord, D. R.; Lindsay Smith, J. R.; Robbins, A. J. *Chem. Soc., Perkin Trans. 2* **1991**, 549–559.
- (17) Chen, S. M.; Su, Y. O. *J. Chem. Soc., Chem. Commun.* **1990**, 491–493.
- (18) Jin, N.; Bourassa, J. L.; Tizio, S. C.; Groves, J. T. *Angew. Chem., Int. Ed.* **2000**, *39*, 3849–3851.
- (19) Bernadou, J.; Fabiano, A.-S.; Robert, A.; Meunier, B. *J. Am. Chem. Soc.* **1994**, *116*, 9375–9376.
- (20) Jin, N.; Ibrahim, M.; Spiro, T. G.; Groves, J. T. *J. Am. Chem. Soc.* **2007**, *129*, 12416–12417.
- (21) Mayer, J. M. *Acc. Chem. Res.* **1998**, *31*, 441–450.
- (22) Shaik, S.; Kumar, D.; de Visser, S. P. *J. Am. Chem. Soc.* **2008**, *130*, 10128–10140.
- (23) Jeong, Y. J.; Kang, Y.; Han, A. R.; Lee, Y. M.; Kotani, H.; Fukuzumi, S.; Nam, W. *Angew. Chem., Int. Ed.* **2008**, *47*, 7321–7324.
- (24) Sheng, X.; Horner, J. H.; Newcomb, M. *J. Am. Chem. Soc.* **2008**, *130*, 13310–13320.
- (25) De Angelis, F.; Jin, N.; Car, R.; Groves, J. T. *Inorg. Chem.* **2006**, *45*, 4268–4276.
- (26) Shimanovich, R.; Groves, J. T. *Arch. Biochem. Biophys.* **2001**, *387*, 307–317.
- (27) Balcells, D.; Raynaud, C.; Crabtree, R. H.; Eisenstein, O. *Inorg. Chem.* **2008**, *47*, 10090–10099.
- (28) Altun, A.; Shaik, S.; Thiel, W. *J. Am. Chem. Soc.* **2007**, *129*, 8978–8987.
- (29) Ogliaro, F.; de Visser, S. P.; Groves, J. T.; Shaik, S. *Angew. Chem., Int. Ed.* **2001**, *40*, 2874–2878.

JA903394S